ADVANCED MATERIALS TECHNOLOGIES

Supporting Information

for *Adv. Mater. Technol.*, DOI: 10.1002/admt.201700135

An Additive Millimeter-Scale Fabrication Method for Soft Biocompatible Actuators and Sensors

Sheila Russo, Tommaso Ranzani, Conor J. Walsh, and Robert J. Wood*

Supplementary Information for

An additive millimeter-scale fabrication method for soft biocompatible actuators and sensors

Sheila Russo,* Tommaso Ranzani, Conor J. Walsh, Robert J. Wood

*Corresponding author. E-mail: srusso@seas.harvard.edu.
Harvard John A. Paulson School of Engineering and Applied Sciences, Cambridge, MA 02138
Wyss Institute, Harvard University, Cambridge, MA 02138

This PDF file includes:

- Figures S1, S2, S3, and S4
- Tables S1, S2, S3, S4, S5, and S6
- Captions for Movies S1, S2, and S3

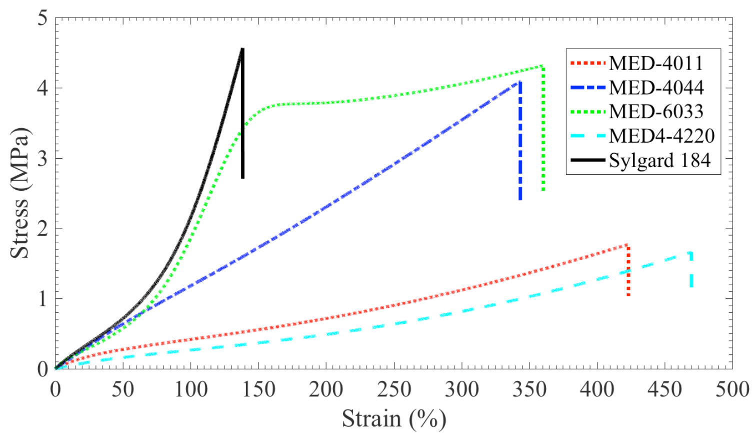

Figure S1: Tensile tests of Sylgard® 184, MED4-4220 (17A durometer), MED-4011 (27A durometer), MED-4044 (40A durometer), and MED-6033 (50A durometer).

Table S1: 3M® 9877 adhesive peel strength on different substrates in comparison with DuPont™ Pyralux® FR0100.

Adhesive	Materials	Mean (N/mm)	St dev (N/mm)	Min (N/mm)	Max (N/mm)
3M™ 9877	FR4/Cu	1.37	0.12	1.24	1.55
3M™ 9877	FR4/PI	1.36	0.21	1.13	1.61
3M™ 9877	SS/Cu	1.11	0.04	1.06	1.13
3M™ 9877	SS/PI	1.28	0.1	1.2	1.42
DuPont™ FR0100®	Cu	1.6	N.A.	N.A.	N.A.

Table S2: Contact angle measurements on pristine, O_2 plasma treated, and amine-functionalized surfaces: stainless steel (SS), fiber reinforced epoxy resin (FR4), copper (Cu), and polyimide (PI). Each value reported is the average and the corresponding standard deviation of a minimum of five measurements.

Material	Pristine	O_2 plasma	APTES
SS	74.9° ± 1.3° 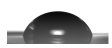	8.1° ± 2.0° 	39.2° ± 2.6° 
FR4	89.5° ± 1.6° 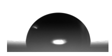	21.6° ± 1.8° 	26.7° ± 1.9° 
Cu	75.4° ± 1.0° 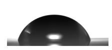	7.7° ± 1.1° 	49.3° ± 0.9° 
PI	79.4° ± 1.7° 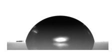	14.1° ± 0.9° 	34.2° ± 1.2° 

Table S3: Chemical bonding method peel strength.

Materials	Mean (N/mm)	St dev (N/mm)	Min (N/mm)	Max (N/mm)
MED4-4220/FR4	1.17	0.1	1.09	1.31
MED4-4220/Cu	0.8	0.07	0.72	0.89
MED4-4220/SS	1.12	0.09	1.03	1.22
MED4-4220/PI	1.01	0.13	0.89	1.17
MED-6033/FR4	0.95	0.05	0.90	1.01
MED-6033/Cu	0.81	0.03	0.77	0.84
MED-6033/SS	0.78	0.01	0.77	0.79
MED-6033/PI	0.71	0.04	0.66	0.75

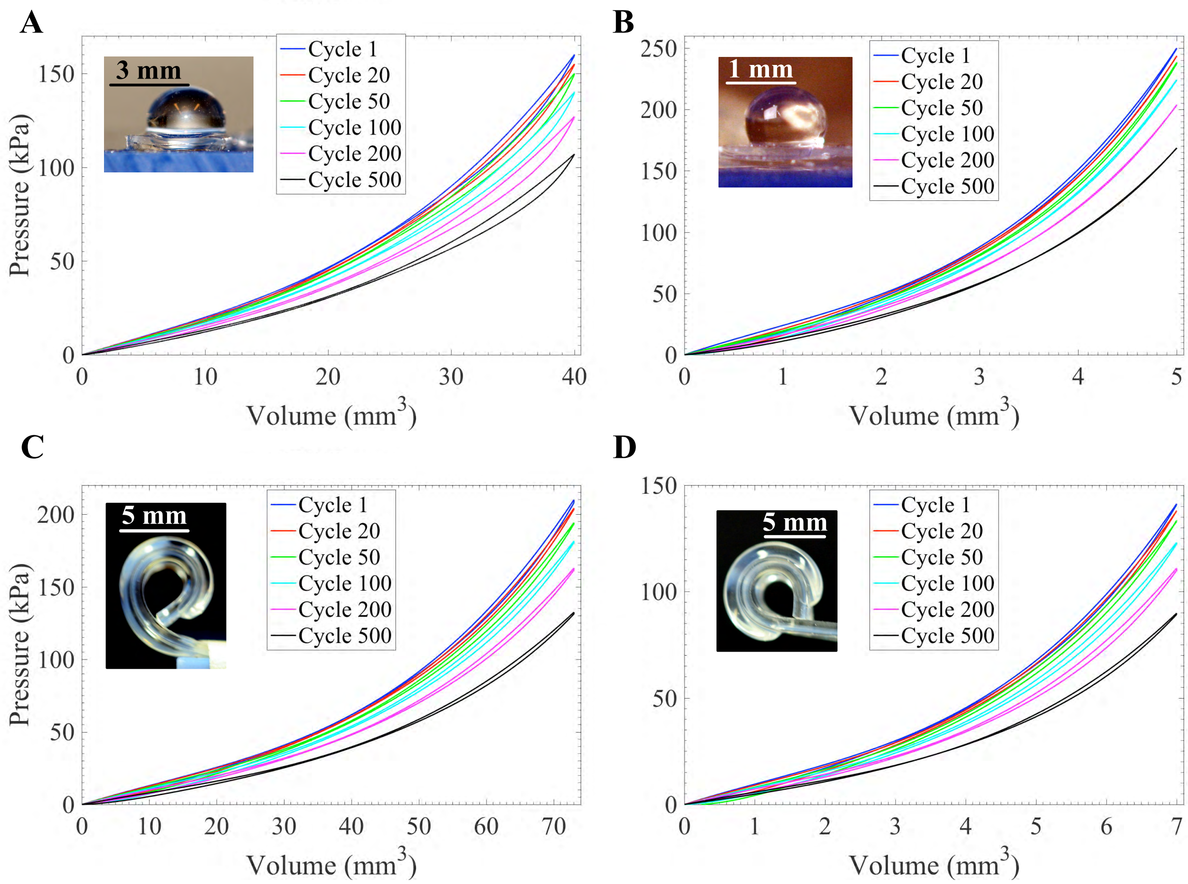

Figure S2: Fatigue tests. (A) AFS at 5 mm scale. (B) AFS at 1.25 mm scale. (C) BFS at 5 mm scale. (D) BFS at 1.25 mm scale. The plots show PV hysteresis curves for the first cycle of inflation and deflation and after 20, 50, 100, 200, and 500 cycles. The captions in the plot show the actuators when fully expanded/bent.

Table S4: Reduction of pressure necessary to fully inflate actuators after cyclic testing reported in percentage with respect to the first cycle.

Cycle	AFS 5 mm	AFS 1.25 mm	BFS 5 mm	BFS 1.25 mm
20	3.13 %	2.52 %	3.19 %	2.27 %
50	6.25 %	5.04 %	7.95 %	5.52 %
100	12.50 %	10.40 %	14.05 %	13.31 %
200	20.63 %	18.52 %	23.10 %	22.17 %
500	33.13 %	32.52 %	37.52 %	36.37 %

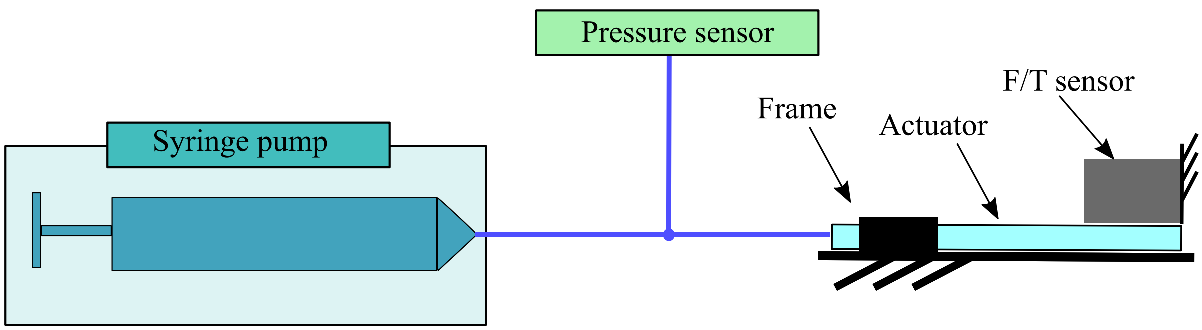

Figure S3: Scheme of the experimental setup used for the blocked force/torque testing.

Table S5: Actuators stiffness. Bending stiffness values for the BFS, IMJ, and EMJ actuators computed at different scales and different test conditions: at rest (0°) condition and actuated (45°) condition.

Actuator type	Scale (mm)	k @ 0°(N/m)	k @ 45°(N/m)
IMJ	5	92.4	70.7
	2.5	105.7	70
	1.25	128.1	77.2
EMJ	5	20	42.3
	2.5	27.7	29.5
	1.25	35.3	40
BFS	5	1.4	7
	2.5	1.4	6.6
	1.25	1.4	6.4

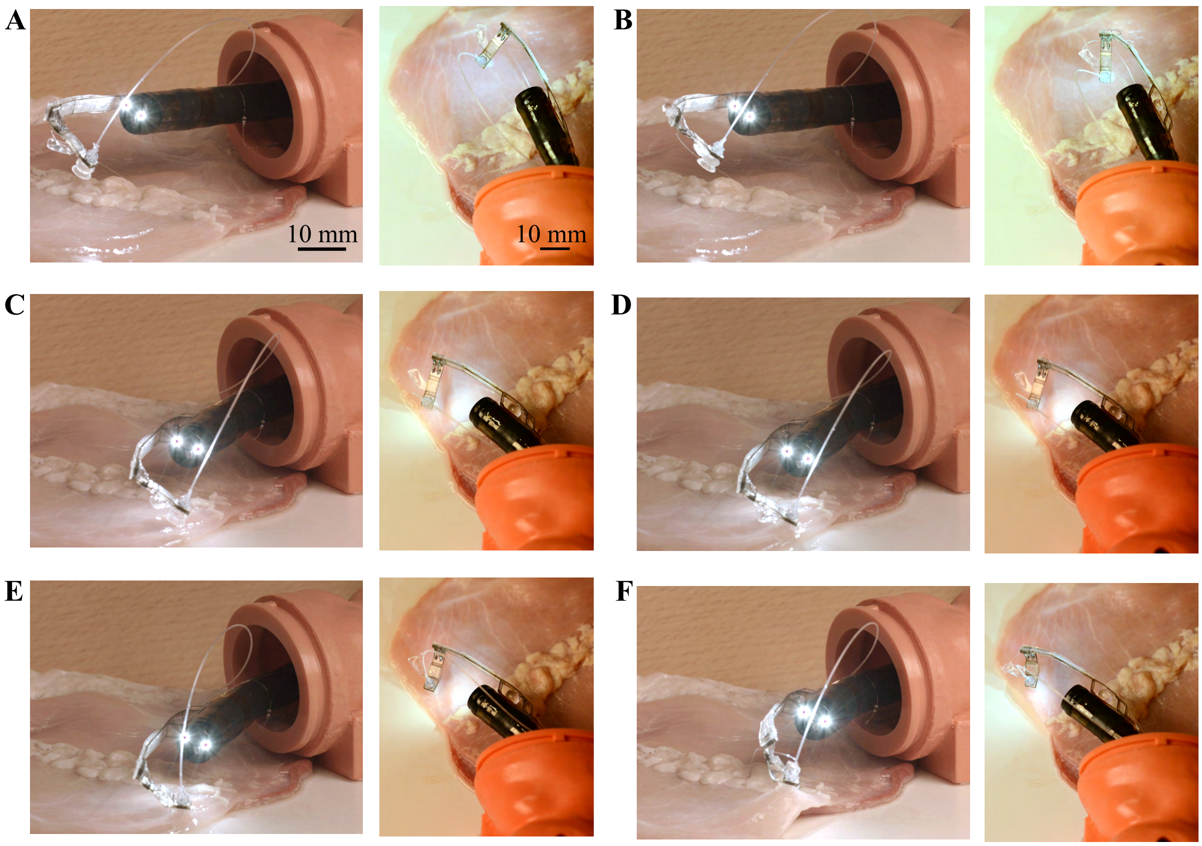

Figure S4: Soft pop-up arm *ex-vivo* test on porcine stomach. The arm is mounted on a flexible endoscope and passed through a gastrointestinal tract anthropomorphic phantom. For each step, side and top views are shown. (A) Initial position. (B) Activation of expansion and yaw DOFs. (C) The endoscope is moved to position the end-effector on a location of interest. (D) The gripper is activated (by turning on vacuum) and the tissue is grasped. (E) Activation of the pitch DOF to counter-tract the tissue. (F) Additional tissue tensioning combining pitch DOF with endoscope movement.

Table S6: Summary of AFS characteristics.

Actuator type	Scale (mm)	Blocked force (N)	Max deflection (mm)	Max speed (mm/s)	Max work output (J)	Max power output (W)	Max power density (W/m^3)	Max power density (W/kg)
AFS	5	1.54	3	1.7	4.62×10^{-3}	2.72	4.59×10^{7}	3.4×10^{4}
	2.5	0.49	2.2	2.6	1.09×10^{-3}	0.42	2.83×10^{7}	1.23×10^{4}
	1.25	0.17	1.64	2.8	0.28×10^{-3}	0.1	1.71×10^{7}	4.98×10^{3}

Movie S1

This movie shows the two soft fluidic micro actuators (SFMA): axial fully soft actuator (AFS) and bending fully soft actuator (BFS) at 5, 2.5, and 1.25 mm scales, during inflation and deflation at the maximum speed.

Movie S2

This movie shows the soft pop-up actuators: internal micro-balloon joint (IMJ) and external micro-balloon joint (EMJ) at 5, 2.5, and 1.25 mm scales, during inflation and deflation at the maximum speed.

Movie S3

This movie shows the *ex-vivo* test performed on a porcine stomach of the multiarticulated soft pop-up robotic arm. The arm is mounted on top of a flexible endoscope (Olympus CF-100TL) and passed through a gastrointestinal tract anthropomorphic phantom (AK107, Lower GI Endoscopy Simulator, Adam Rouilly, UK). Three different points of view of the experiment are shown: side, top, and endoscope camera view. At first, the expansion degree of freedom is activated to move the arm with respect to the endoscope vision system (surgical triangulation). Then, the yaw DOF is activated together with the endoscope tip to move the arm with respect to the tissue and reach a desired location (e.g. a lesion). At this point, the soft suction-based gripper (*25*) is activated (by turning on vacuum) and tissue is grasped. Subsequently, the pitch DOF is used to counter-tract the tissue and additional tensioning is achieved exploiting the endoscope movement. Finally, tissue is released by deactivating the soft gripper (turning off vacuum) and the arm is moved back to the original position.